THE JOURNAL OF BIOLOGICAL CHEMISTRY VOL. 290, NO. 4, pp. 2455–2465, January 23, 2015

Crystal Structure of LGR4-Rspo1 Complex

*INSIGHTS INTO THE DIVERGENT MECHANISMS OF LIGAND RECOGNITION BY LEUCINE-RICH REPEAT G-PROTEIN-COUPLED RECEPTORS (LGRs)**

Received for publication, July 23, 2014, and in revised form, December 3, 2014 Published, JBC Papers in Press, December 5, 2014, DOI 10.1074/jbc.M114.599134

Jin-Gen Xu[‡1], Chunfeng Huang[‡1], Zhengfeng Yang[§], Mengmeng Jin[‡], Panhan Fu[‡], Ni Zhang[‡], Jian Luo[§], Dali Li[§], Mingyao Liu[§], Yan Zhou[‡2], and Yongqun Zhu[‡3]

From the [‡]Life Sciences Institute and Innovation Center for Cell Biology, Zhejiang University, Hangzhou, Zhejiang 310058 and the [§]Shanghai Key Laboratory of Regulatory Biology, Institute of Biomedical Sciences and School of Life Sciences, East China Normal University, Shanghai 200241, China

Background: LGR receptors play important roles in many developmental processes.
Results: The structure of human LGR4-Rspo1 complex was solved.
Conclusion: Diverse mechanisms are utilized by LGRs in ligand recognition.
Significance: Our structures are important for potential drug design.

Leucine-rich repeat G-protein-coupled receptors (LGRs) are a unique class of G-protein-coupled receptors characterized by a large extracellular domain to recognize ligands and regulate many important developmental processes. Among the three groups of LGRs, group B members (LGR4–6) recognize R-spondin family proteins (Rspo1–4) to stimulate Wnt signaling. In this study, we successfully utilized the "hybrid leucine-rich repeat technique," which fused LGR4 with the hagfish VLR protein, to obtain two recombinant human LGR4 proteins, $LGR4_{15}$ and $LGR4_{9}$. We determined the crystal structures of ligand-free $LGR4_{15}$ and the $LGR4_{9}$-Rspo1 complex. LGR4 exhibits a twisted horseshoe-like structure. Rspo1 adopts a flat and β-fold architecture and is bound in the concave surface of LGR4 in the complex through electrostatic and hydrophobic interactions. All the Rspo1-binding residues are conserved in LGR4–6, suggesting that LGR4–6 bind R-spondins through an identical surface. Structural analysis of our LGR4-Rspo1 complex with the previously determined LGR4 and LGR5 structures revealed that the concave surface of LGR4 is the sole binding site for R-spondins, suggesting a one-site binding model of LGR4–6 in ligand recognition. The molecular mechanism of LGR4–6 is distinct from the two-step mechanism of group A receptors LGR1–3 and the multiple-interface binding model of group C receptors LGR7–8, suggesting LGRs utilize the divergent mechanisms for ligand recognition. Our structures, together with previous reports, provide a comprehensive understanding of the ligand recognition by LGRs.

G-protein-coupled receptors (GPCRs),[4] a large group of cell surface receptors, play key roles in many cellular processes. GPCRs generally contain a seven-transmembrane (7TM) domain responsible for ligand binding and downstream G-protein activation. Leucine-rich repeat G-protein-coupled receptors (LGRs) are a unique class of GPCRs characterized by a large extracellular domain (ectodomain) that harbors multiple copies of leucine-rich repeat (LRR) (1). The ectodomain mediates ligand binding to modulate downstream intracellular signaling pathways. LGRs are subdivided into three subgroups (group A, B, and C), according to their sequence similarities (1, 2). Group A LGRs have seven to nine LRRs in their ectodomain and long hinge regions connecting the LRR domain to the 7TM domain. Group A receptors include LGR1, LGR2, and LGR3, which recognize follicle-stimulating hormone (FSH), luteinizing hormone, and thyroid-stimulating hormone, respectively (3, 4). Group C LGRs have similar numbers of LRRs but contain a low density lipoprotein receptor class A domain motif at the N terminus and a short hinge region between the LRR domain and the 7TM domain. Group C LGRs include the relaxin receptor LGR7 and INSL3 (insulin-like peptide 3) receptor LGR8 (1, 3, 4). The molecular mechanisms of ligand recognition by group A and C receptors have been extensively studied and are relatively well understood.

The group B receptors include LGR4, LGR5, and LGR6, which are characterized by a long ectodomain containing 17 LRR repeats (2, 4). LGR4–6 share ~50% sequence identity and play key roles in stem cell development. The 17 LRR repeats of the LGR4–6 receptors are flanked by the N-terminal cysteine-rich LRRNT region and the C-terminal cysteine-rich LRRCT region (4). The ligands of LGR4–6 remained unidentified for a long time. Recently, the secreted R-spondin proteins (Rspo1–4) were identified as the endogenous ligands for the group receptors

* This work was supported by China's Fundamental Research Funds for the Central Universities, Research Grants 31370722 and 81322024 from the NSFC, Grant LR13C05001 from Natural Science Foundation of Zhejiang Province, and Grant J20130639 from Zhejiang University K. P. Chao's High Technology Development Foundation (to Y. Zhu).
The atomic coordinates and structure factors (codes 4QXE and 4QXF) have been deposited in the Protein Data Bank (http://wwpdb.org/).
[1] Both authors contributed equally to this work.
[2] To whom correspondence may be addressed: Life Sciences Institute, Zhejiang University, 866 Yuhangtang Rd., Hangzhou, Zhejiang 310058, China. Tel.: 86-571-88206740; E-mail: zhouyanlsi@zju.edu.cn.
[3] To whom correspondence may be addressed: Life Sciences Institute, Zhejiang University, 866 Yuhangtang Rd., Hangzhou, Zhejiang 310058, China. Tel.: 86-571-88206122; Fax: 86-571-88981337; E-mail: zhuyongqun@zju.edu.cn.

[4] The abbreviations used are: GPCR, G-protein-coupled receptor; LGR, leucine-rich repeat G-protein-coupled receptor; LRR, leucine-rich repeat; FSH, follicle-stimulating hormone; FSHR, FSH receptor; TSHR, thyroid-stimulating hormone receptor; PDB, Protein Data Bank; 7TM, seven-transmembrane; CM, conditional medium; Rspo, R-spondin; Fu-CRD, furin-like cysteine-rich.

to stimulate the Wnt signaling pathways, regulating cell proliferation, differentiation, and adult stem cell maintenance (5, 6).

The R-spondin (Rspo) family of proteins include four members (Rspo1–4) and are conserved in vertebrates. R-spondins are involved in numerous developmental processes (7–9), including sex (10, 11), lung, limb, hair follicle (9, 12), and nail development (13–15). The four R-spondin proteins share ~40–60% pairwise sequence homology and adopt a common domain architecture that consists of an N-terminal secretory signal peptide sequence, two tandem furin-like cysteine-rich (Fu-CRD) domains, a thrombospondin type I repeat (TSP) domain, and a C-terminal basic amino acid-rich (BR) domain. Among the four subdomains, the two central tandem Fu-CRD domains have been demonstrated to be essential and sufficient for R-spondin stimulation of Wnt signaling (16–18). Previous studies had revealed that the ectodomains of LGR4–6 specifically recognize the two Fu-CRD domains of R-spondins (16, 17).

Although LGR4–6 contain a 7TM domain as the group A and group C receptors, the stimulation of Wnt signaling by LGR4–6 was found to be independent of downstream G-protein activation, suggesting the functional difference of LGR4–6 from LGR1–3 and LGR7–8. Here, we successfully utilized the "hybrid LRR technique" to obtain human LGR4 proteins from insect cells. We determined the crystal structure of human LGR4 alone at a resolution of 2.2 Å, as well as its complex structure with Rspo1 at a resolution of 2.25 Å. Our studies, together with the previously determined structures (19–22), suggest that LGR4–6 recognize R-spondins via a distinct mechanism from those of LGR1–3 and LGR7–8.

EXPERIMENTAL PROCEDURES

Plasmids, Reagents, and Mutagenesis—To express human LGR4 and Rspo1 in insect cells, the $LGR4_{15}$ and $LGR4_9$ hybrids (Fig. 1) were cloned into the pFastBac1 vector (Invitrogen) with a gp67 secretory signal peptide at the N terminus and a Fc-9×His tag with a tobacco etch virus protease cleavage site at the C terminus. The two furin-like cysteine-rich regions of Rspo1 (residues 34–135) were cloned into the pFastBac1 vector with an N-terminal gp67 signal peptide. For TOP/FOPFlash assays, full-length wild-type and mutant LGR4 were cloned into the pCDNA4 vector with a CD8 secretory signal peptide and a FLAG tag at the N terminus. Full-length Rspo1 and its mutants were cloned into the pCDNA4 vector with a C-terminal HA tag. All site-directed mutageneses were performed with the standard overlap-extension PCR method, and all plasmids were verified by DNA sequencing.

Protein Expression and Purification—Recombinant proteins were expressed in Sf9 insect cells using the Bac-to-Bac baculovirus expression system (Invitrogen). $LGR4_{15}$ and $LGR4_9$ recombinant proteins were purified from cell medium using nickel-nitrilotriacetic acid resins. After tobacco etch virus protease digestion to remove the C-terminal Fc-9×His tag, the proteins were further purified by size exclusion chromatography using Superdex 200 10/300 GL column (GE Healthcare). Both purified proteins were concentrated to 10 mg/ml in the Tris-HCl buffer containing 50 mM Tris-HCl, pH 8.0, and 150 mM NaCl for crystallization. To obtain the recombinant $LGR4_9$-Rspo1 complex, Sf9 cells were co-infected with baculoviruses encoding $LGR4_9$ and human Rspo1 (residues 34–135). After 60 h post-infection, the $LGR4_9$-Rspo1 complex was purified from cell medium using nickel-nitrilotriacetic acid column and further purified using a Mono Q column (GE Healthcare). The purified $LGR4_9$-Rspo1 complex was concentrated to 40 mg/ml in the buffer containing 50 mM Tris-HCl, pH 8.0, and 150 mM NaCl for crystallization.

Crystallization and Data Collection—All crystallization experiments were carried out with the hanging-drop vapor diffusion method at 16 °C. In initial crystal screening, crystals of $LGR4_{15}$ and $LGR4_9$ appeared after 3 days. Crystals of $LGR4_{15}$ were selected for structural determination. After extensive optimization, diffraction-qualified crystals of $LGR4_{15}$ were obtained in the well condition containing 0.1 M HEPES, pH 7.5, and 2.0 M ammonium sulfate. Crystals of $LGR4_{15}$ were transferred into the well solution supplemented with 15% glycerol as the cryoprotectant and then flash-cooled into liquid nitrogen for data collection. The $LGR4_9$-Rspo1 complex was crystallized after 7 days in the well solution containing 0.1 M MES, pH 6.5, 0.2 M sodium thiocyanate, and 22% PEG 3350. The crystals were cryoprotected with the well solution supplemented with 20% glycerol in liquid nitrogen. All diffraction data were collected on the BL17U1 beamline of Shanghai Synchrotron Radiation Facility and processed with the HKL-2000 package (23).

Structural Determination—The $LGR4_{15}$ structure was solved with the molecular replacement method using the partial model of LRR repeats from TLR5 (PDB code 3V44) (24) as the search mode in the Phaser program (25) in CCP4 (26). The final structure was refined to 2.2 Å with R_{work}/R_{free} of 20.7%/23.4% in Refmac5 (27).There is one $LGR4_{15}$ molecule in an asymmetric unit. The $LGR4_9$-Rspo1 complex structure was solved with the molecular replacement method using $LGR4_{15}$ and VLR (residues 129–200) as the search modes. The final structure of $LGR4_9$-Rspo1 complex was refined to 2.25 Å with R_{work}/R_{free} of 21.3%/24.2% in Refmac5. There are two $LGR4_9$-Rspo1 complex molecules in an asymmetric unit. Because of the lack of electron density, the N-terminal 18 residues and C-terminal 5 residues of Rspo1 were missed in the final complex model. All model building was performed in Coot (28). All structures were checked with the program Procheck (29). All structural pictures were prepared in PyMOL. Statistics of data collection and refinement are listed in Table 1.

TOP/FOPFlash Assays—TOP/FOPFlash assays were carried out similarly as described (30). To test the effect of Rspo1 mutations, HEK293T cells cultured in 12-well plates were transfected with 500 ng of Super 8× TOPFlash or FOPFlash firefly luciferase reporter, 10 ng of *Renilla* luciferase reporter, and 750 ng of wild-type LGR4 plasmids. Wild type and mutant Rspo1 conditional medium (CM) were prepared by culturing HEK293T cells in 6-well plates, which were transiently transfected with 2 μg of Rspo1 variant plasmids in each well. Wnt3a CM was obtained from mouse L cells stably expressing Wnt3a. After a 24-h co-stimulation by Wnt3a and wild-type or mutant Rspo1 CM, the transfected HEK293T cells were harvested for Dual-Luciferase® reporter assays by using the Dual-Glo luciferase assay kit (Promega). To test the effect of LGR4 mutations on the Rspo1 stimulation of Wnt signaling, HEK293T cells cul-

tured in 12-well plates were transfected with 500 ng of Super 8× TOPFlash or FOPFlash firefly luciferase reporter, 10 ng of *Renilla* luciferase reporter, and 1 μg of wild-type or mutant LGR4 plasmids. After stimulation for 24 h with Wnt3a and wild-type Rspo1 CM, the cells were harvested for Dual-Luciferase reporter assays. The relative TOP/FOPFlash luciferase activities presented were normalized against the levels of vector control.

RESULTS AND DISCUSSION

Production of Recombinant Human LGR4 and LGR4-Rspo1 Complex Proteins—The ectodomain of human LGR4 includes residues 28–528. The two central tandem Fu-CRD domains of human Rspo1, which are required for binding the LGRs, include residues 34–135. When expressed in insect cells, the human LGR4 ectodomain severely aggregated during purification. To enhance the solubility and stability of the LGR4 ectodomain, we designed LGR4 chimeras that contain the LRR repeats of the LGR4 ectodomain and the hagfish VLR protein using the hybrid LRR technique, which was previously used to facilitate the soluble expression and crystallization of TLR4 (Fig. 1*A*) (31). Previous studies have suggested that the N-terminal residues of LGRs are important for interaction with R-spondins (16). Therefore, we attempted to fuse the N-terminal LRR repeats of LGR4 with the C-terminal regions of the hagfish VLR protein according to the "*LXXLXLXXNXLXXL*" consensus sequence of LRR modules.

After many attempts, we successfully expressed and crystallized two LGR4 ectodomain fusion proteins, $LGR4_{15}$ and $LGR4_9$ (Fig. 1, *A* and *B*). In $LGR4_{15}$, the N-terminal 15 LRRs of LGR4 (residues 28–396) were fused with the VLR residues 131–200 (VLR_A). In $LGR4_9$, the N-terminal nine LRRs of LGR4 (residues 28–253) were fused with the C-terminal 72 residues of VLR (residues 129–200, VLR_B). Both chimeric proteins formed stable protein complexes with Rspo1 during purification, suggesting that our designed LGR4 proteins contain the entire Rspo1-binding region. $LGR4_{15}$ crystals were selected for structural determination because the construct contains more residues of LGR4. The $LGR4_{15}$ structure was finally refined to 2.2 Å with R_{work}/R_{free} values of 20.7%/23.4% (Table 1). Because $LGR4_{15}$ precipitated in polyethylene glycols, which are extensively used in the crystallization of protein complexes, we co-expressed $LGR4_9$ with the two central tandem Fu-CRD domains of Rspo1 (residues 34–135) in insect cells to assemble the receptor-ligand complex for crystallization. We successfully crystallized the $LGR4_9$-Rspo1 complex and determined its structure to 2.25 Å with high geometry quality (Table 1). Details of the data collection and structural refinement statistics are summarized in Table 1.

Human LGR4 Ectodomain Structure—The final model of the ligand-free $LGR4_{15}$ structure includes all residues of the designed hybrid construct. The overall architecture of $LGR4_{15}$ adopts a typical twisted solenoid-like structure (Fig. 1*B*). As expected, the central 15 LRR repeats of $LGR4_{15}$ are flanked by the N-terminal LRRNT (residues 28–57) and the C-terminal VLR module (Fig. 1*B*). In total, 17 β-strands are present in the $LGR4_{15}$ structure, of which 15 originate from the LRR repeats, one from LRRNT, and one from VLR. The 17 β-strands form

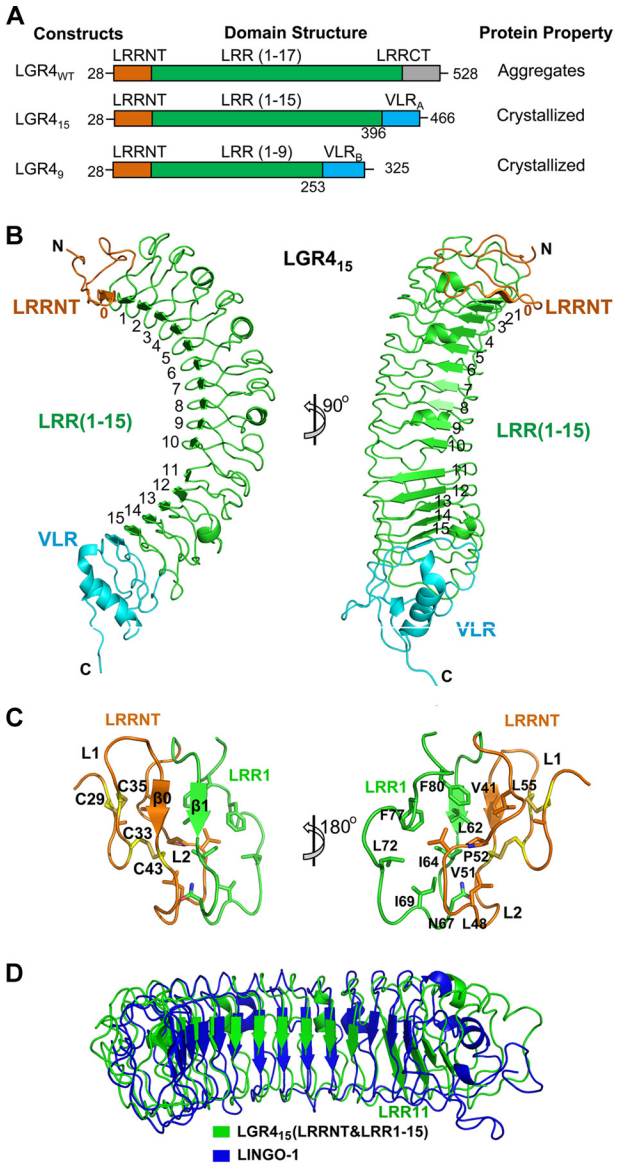

FIGURE 1. **Crystal structure of $LGR4_{15}$.** *A,* LGR4 constructs designed by using the hybrid LRR technique to enhance protein stability. The ectodomain of LGR4 contains LRRNT (*orange*), LRR (*green*), and LRRCT (*gray*). $LGR4_{15}$ was designed by fusing the N-terminal LRRNT and 15 LRR repeats with a hagfish VLR_A module (*cyan*, residues 131–200, Asp-131 and Thr-132 were mutated to alanine and serine). $LGR4_9$ was designed by fusing the N-terminal LRRNT and nine LRR repeats with a VLR_B module (*cyan,* residue 129–200). *B,* overall structure of $LGR4_{15}$. The central 15 LRR repeats of $LGR4_{15}$ are colored in *green* and labeled as indicated. The LRRNT and the VLR module are colored in *orange* and *cyan*, respectively. *C,* structure of LRRNT and its interaction with LRR1. LRRNT and LRR1 are colored in *orange* and *green*, respectively. The four cysteine residues are shown as *yellow sticks* and form two disulfide bonds (Cys-29–Cys-35, Cys-33–Cys-43) in LRRNT. *D,* structural comparison of LINGO-1 and $LGR4_{15}$ (LRRNT and LRR(1–15)). $LGR4_{15}$ and LINGO-1 are colored in *blue* and *yellow*, respectively. The LRR11 repeat of $LGR4_{15}$ is labeled.

the inner concave surface of $LGR4_{15}$, which interacts with Rspo1 in the LGR4-Rspo1 complex structure (details below). The outer convex surface of $LGR4_{15}$ is composed of 10 linking loops and four short linking α-helices from the LRR repeats (Fig. 1*B*).

At the $LGR4_{15}$ N terminus, LRRNT consists of two loops (L1 and L2) and one β-strand (β0). It forms a capping structure to protect the first LRR repeat (LRR1) from solvent exposure (Fig.

TABLE 1
Data collection and refinement statistics

	$LGR4_{15}$	$LGR4_9$-Rspo1
Data collection		
Space group	$I2_13$	$P2_1$
Cell dimensions		
a, *b*, *c* (Å)	173.76, 173.76, 173.76	44.87, 137.91, 82.56
α, β, γ (°)	90.00, 90.00, 90.00	90.00, 100.13, 90.00
Wavelength	1.0000	0.97925
Resolution (Å)[a]	50-2.20 (2.28-2.20)	50-2.20 (2.28-2.25)
R_{sym} or R_{merge}	0.116 (0.610)	0.090 (0.650)
$I/\sigma I$	56.9 (13.1)	37.7 (11.3)
Completeness (%)	100 (100)	98.8 (98.3)
Redundancy	28.1 (27.4)	5.0 (5.2)
Refinement		
Resolution (Å)	50-2.2	50-2.25
No. of reflections	41,816	43,609
R_{work}/R_{free}(%)[b]	20.7/23.4	21.3/24.2
No. of atoms		
Protein	3,477	5,859
Water/ligand	267	291
B-factors (Å^2)		
Protein	30.34	28.49
Water/ligand	35.04	17.40
Root mean square deviations		
Bond lengths (Å)	0.007	0.009
Bond angles (°)	1.171	1.267
Ramachandran plot		
Preferred regions(%)	92.6	92.9
Allowed regions(%)	7.4	7.1

[a] The data for the highest resolution shell are shown in parentheses.
[b] R_{free} is calculated using 10% of the total number of reflections.

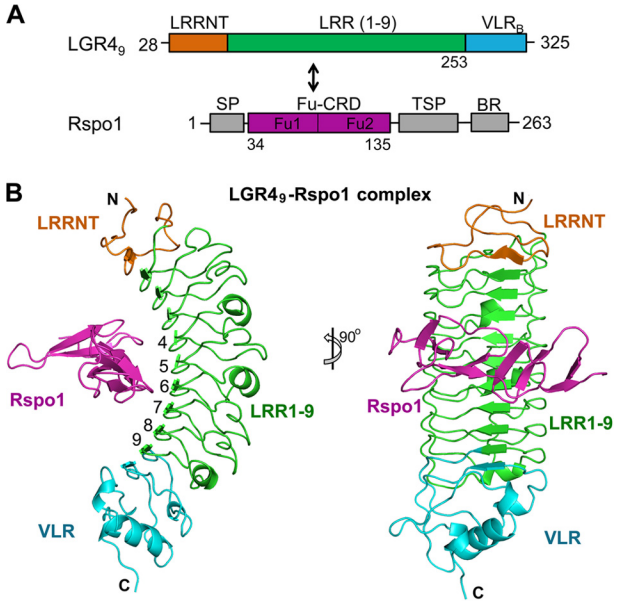

FIGURE 2. **Structure of the $LGR4_9$-Rspo1 complex.** *A*, domain structures of $LGR4_9$ and Rspo1. $LGR4_9$ and the two central furin-like domains (*Fu1* and *Fu2*, colored in *purple*) of Rspo1 were co-expressed for the LGR4-Rspo1 complex. *B*, structure of the $LGR4_9$-Rspo1 complex. Rspo1 is colored in *purple*. The central nine LRR repeats of $LGR4_9$ are colored in *green*. The LRRNT and VLR subdomains of $LGR4_9$ are colored in *orange* and *cyan*, respectively.

1*C*). LRRNT binds to LRR1 through extensive interactions. The β0 strand of LRRNT forms a parallel β-sheet with β1 of LRR1. The hydrophobic residues Val-41, Leu-48, Pro-52, and Leu-55 from β0 and L2 in LRRNT strongly stack with Leu-62, Ile-64, Asn-67, Ile-69, Leu-72, Phe-77, and Phe-80 of LRR1 (Fig. 1*C*). LRRNT contains four cysteine residues, which form two disulfide bonds (Cys-29–Cys-35 and Cys-33–Cys-43) to stabilize the L1 loop. These cysteine residues are conserved in LGR5 and LGR6, suggesting that the cysteine residues play important roles in maintaining the LRRNT cap-like structure. At the C terminus of $LGR4_{15}$, the VLR protein contains one α-helix, one β-strand, and three loops. It adopts the identical conformation as reported previously (Fig. 1*B*) (31). VLR stabilizes the LGR4 C terminus through a parallel β-sheet and extensive hydrophobic interactions with LRR15.

A structural homology search using the $LGR4_{15}$ structure (LRRNT and LRR(1–15)) as the bait in the Dali server (32) revealed that $LGR4_{15}$ shares significant structural similarities with several LRR receptors, including LINGO-1, TLR2, TLR4, and TLR5 (24, 31, 33, 34). $LGR4_{15}$ exhibits the highest structural similarity to the extracellular LRR subdomain of the human neuron co-receptor LINGO-1 (PDB code 2ID5) with a Z-score value of 32.4 and a root mean square deviation value of 4.4 Å for 347 aligned residues (Fig. 1*D*) (34). LINGO-1 forms a ternary complex with NgR1 and p75 to constitute the Nogo receptor for myelin and mediates the inhibition of axonal growth (34). Although the overall structure of $LGR4_{15}$ is highly similar to the extracellular LRR subdomain of LINGO-1, the C terminus of $LGR4_{15}$ (LRR11–15) is largely different from that of LINGO-1 (Fig. 1*D*).

Structure of the Human LGR4-Rspo1 Complex—The recombinant LGR4-Rspo1 complex for crystallization was prepared from the co-expression of $LGR4_9$ with the two central Fu-CRD domains of Rspo1 in insect cells (Fig. 2*A*). $LGR4_9$ formed a stable 1:1 complex with Rspo1 during size exclusion chromatography. We successfully crystallized the $LGR4_9$-Rspo1 complex and determined its structure by the molecular replacement method using $LGR4_{15}$ and VLR as the search models. In the final structural model of the $LGR4_9$-Rspo1 complex, there are two $LGR4_9$-Rspo1 complex copies related by the noncrystallography symmetry in an asymmetric unit. Because the two complex molecules adopt identical conformation, hereafter, we describe one of them in our structural analysis.

Like the ligand-free $LGR4_{15}$ structure, Rspo1-bound $LGR4_9$ adopts a short twisted solenoid-like structure and contains the N-terminal LRRNT, the central nine leucine-rich repeats (LRR1–9), and the C-terminal hagfish VLR region (Fig. 2*B*). All of the residues in the designed $LGR4_9$ chimera are included in the final $LGR4_9$ model. In the complex, Rspo1 horizontally crosses the inner concave surface of $LGR4_9$ from one side to the other side and binds to the concave surface through extensive interactions with the central six LRR repeats (LRR4–9) of $LGR4_9$ (Fig. 2*B*).

Rspo1 Structure in the LGR4-Rspo1 Complex—Rspo1 in complex with LGR4 is composed of eight β-strands that form an elongated and flat overall architecture (Fig. 3*A*). The final Rspo1 model only includes the central 78 residues, which constitute eight β-strands (β1–β8) in the structure (Fig. 3*B*). The N-terminal 18 residues (Ala-34–Asn-51) and the C-terminal five residues (Glu-131–Ala-135) of Rspo1 are missing in the structure due to lack of electron density. These residues are not conserved in the four R-spondin proteins (Fig. 3*B*) and do not participate in any crystal contact.

The eight Rspo1 β-strands constitute four tandem β-hairpins in the order of β2-β1, β4-β3, β5-β6, and β8-β7. Each hairpin contains a two-stranded antiparallel β-sheet and a linking loop. The N-terminal two hairpins (β2-β1 and β4-β3) are longer than the C-terminal hairpins (β5-β6 and β8-β7) (Fig.

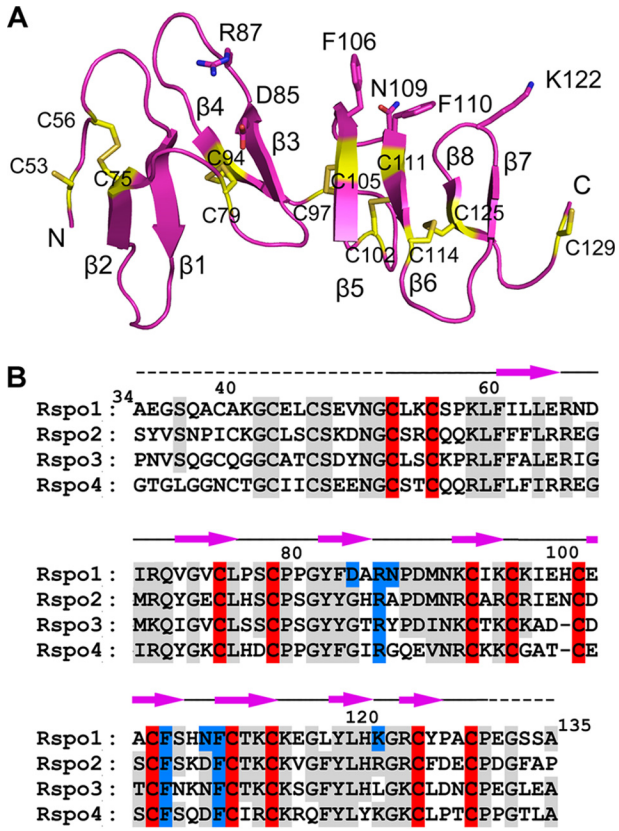

FIGURE 3. **Rspo1 structure in the LGR4$_9$-Rspo1 complex.** *A,* structure of Rspo1. The LGR4-binding residues are shown as *sticks*. The Fu1 subdomain includes the first four β-strands (*β1–β4*). The Fu2 subdomain includes the C-terminal four β-strands (*β5–β8*). All cysteine residues are shown as *yellow sticks* and are labeled as indicated. *B,* sequence alignment of human Rspo1–4. The residues conserved in Rspo1–4 are colored in *gray*. The conserved cysteine residues are specifically highlighted in *red*. The LGR4-binding residues of Rspo1 are highlighted in *blue*. The missed residues in the Rspo1 final model are marked with *dashed lines* above the sequences.

3*A*). The linking loops of the *β*4-*β*3, *β*5-*β*6, and *β*8-*β*7 hairpins, which are located on the same side of Rspo1, are responsible for binding LGR4 in the complex structure. In total, 12 cysteine residues are present in the Rspo1 structure, 10 of which form five disulfide bonds (Cys-56–Cys-75, Cys-79–Cys-94, Cys-97–Cys-105, Cys-102–Cys-111, and Cys-114–Cys-125) (Fig. 3*B*). These disulfide bonds bridge the adjacent hairpins or linking loops to maintain the elongated Rspo1 structure.

Rspo2–4 share high sequence homology with Rspo1 in their furin-like domains (Fig. 3*B*) (7, 18), suggesting that the furin-like domains of Rspo2–4 also adopt the elongated flat *β*-fold structures similar to Rspo1. The 10 cysteine residues of Rspo1, which form five disulfide bonds within the hairpins, are highly conserved in all R-spondin proteins (Fig. 3*B*). Previous clinical studies have revealed that the mutations of the cysteine residues completely disrupt Rspo4 function and cause human autosomal-recessive anonychia (14, 15), suggesting that the five disulfide bonds are critical for maintaining the flat structures of R-spondins. Furin-like cysteine-rich regions also exist in a variety of proteins that are involved in signal transduction via receptor tyrosine kinases (35). Our structural homology search revealed that Rspo1 just exhibits low structural similarity to subdomain IV, the furin-like region of the extracellular region of the EGF receptors HER2, -3, and -4 (36–38). Subdomain IV of EGF receptors has been reported to mediate the inter-receptor dimerization of HER2, -3, and -4 to regulate cellular growth and differentiation (36–38). Rspo1 was superposed with subdomain IV only at its middle hairpin *β*3-*β*4 in structural superimposition.

Interface between LGR4 and Rspo1—In the complex structure, Rspo1 binds to the concave surface of LGR4 through the residues Asp-85, Arg-87, Phe-106, Asn-109, Phe-110, and Lys-122, which are located in the linking loops of the *β*4-*β*3, *β*5-*β*6, and *β*8-*β*7 hairpins, respectively (Fig. 3*A*). The interface between Rspo1 and LGR4 buries a surface area of ~765 Å^2 and involves two differently charged regions on the LGR4 surface, a hydrophilic binding region (region 1) and a hydrophobic binding region (region 2) (Figs. 2*B* and 4*A*).

In the hydrophilic binding region, the positively charged Arg-87 of Rspo1 interacts with an open acidic surface in LGR4. The side chain of Arg-87 in Rspo1 forms three hydrogen bonds with Asn-114, Asp-137, and Asp-161 of LGR4 (Fig. 4*B*). Additionally, Asp-85 of Rspo1 interacts with Arg-135 of LGR4 through a salt bridge. In the hydrophobic binding region, Phe-106 and Phe-110 of Rspo1 form strong interactions with the concave surface of LGR4 (Fig. 4*C*). Phe-106 of Rspo1 stacks with the side chain of Trp-159 of LGR4 and is inserted into a hydrophobic pocket in the concave surface of LGR4, which is formed by Trp-159, Ala-181, Thr-183, and His-207 of LGR4. Phe-110 of Rspo1 interacts with Gln-180, Ala-181, Val-204, and Val-205 of LGR4. In addition to the central hydrophobic interactions, Asn-109 and Lys-122 of Rspo1 interact with Thr-229, Glu-252, and Asn-226 of LGR4 via three hydrogen bonds (Fig. 4*C*).

Mutagenesis Analysis—To examine the interactions observed in the complex structure, we mutated the interacting residues of Rspo1 and LGR4 and carried out the *β*-catenin-driven luciferase reporter assays (Fig. 4, *D* and *E*). A single mutation of the nonconserved Asp-85 of Rpso1 to alanine just had a minor effect on the stimulation of Wnt signaling. But the R87A mutant and the D85A/R87A mutant of Rspo1 could not sufficiently stimulate Wnt signaling (Fig. 4*D*), which indicates that the conserved Arg-87 plays a key role in the LGR4-Rspo1 interaction, and the electrostatic interactions in region 1 are required for Rspo1 recognition by LGR4. The Rspo1 mutations (F106A and F110A) of Phe-106 and Phe-110 at the hydrophobic binding region completely abolished the Rspo1-mediated stimulation of Wnt signaling (Fig. 4*D*), which suggests that the hydrophobic interactions between Rspo1 and LGR4 are also essential for the LGR4-Rspo1 interaction, and the conserved residues Phe-106 and Phe-110 of Rspo1 are critical for the interactions. Different from the F106A and F110A mutations, the N119A and K122A mutants of Rspo1 slightly affected the stimulation of Wnt signaling, suggesting that the nonconserved Asn-119 and Lys-122 of Rspo1 just play supplementary roles in the interactions between Rspo1 and LGR4. The critical residues Arg-87, Phe-106, and Phe-110 of Rspo1 are located in the first furin-like domain (*β*1–*β*4) and the second furin-like domain (*β*5–*β*8), respectively, which well explains why both furin-like domains of R-spondins are required for the recognition by LGRs.

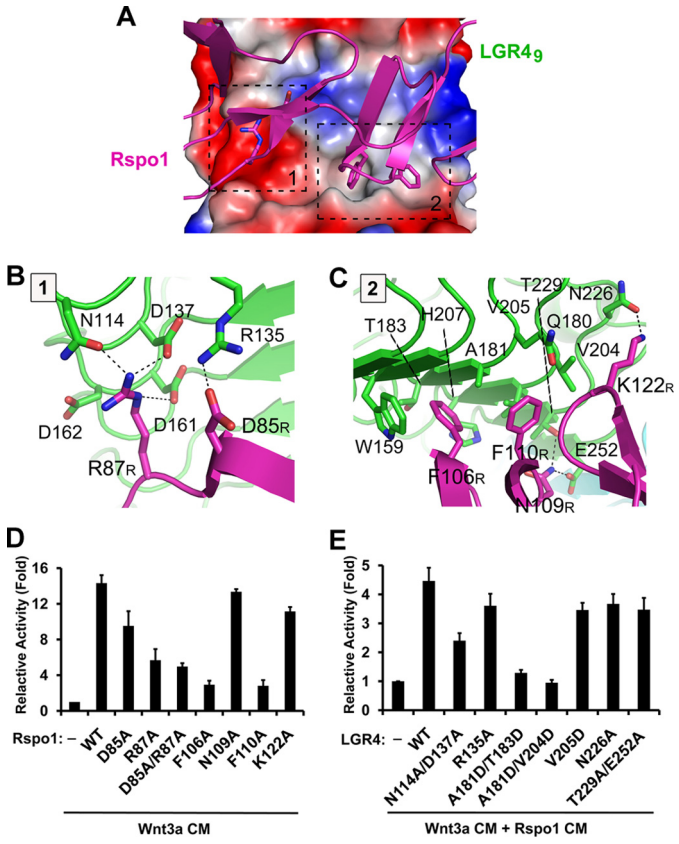

FIGURE 4. **Interface between LGR4 and Rspo1.** *A,* interface between LGR4 and Rspo1. The negatively and positively charged surface and hydrophobic surface of LGR4 are colored in *red, blue,* and *gray*, respectively. The LGR4-interacting residues of Rspo1 are represented as *sticks*. The two interaction regions (regions 1 and 2) in LGR4 are indicated by *black dashed lines*. *B* and *C,* detailed interactions in regions 1 and 2. LGR4 and Rspo1 are colored in *green* and *purple*, respectively. The LGR4-interacting residues in Rspo1 are labeled with the *R* subscripts. *D,* effects of Rspo1 mutations on the stimulation of Wnt signaling. The potentiation of Wnt signaling by Rspo1 mutants was examined using β-catenin-driven Super 8× TOP/FOPFlash luciferase reporter assays. HEK293T cells were transiently transfected with full-length LGR4, TOPFlash, or FOPFlash firefly luciferase, and *Renilla* luciferase plasmids and were then stimulated with the CM of Rspo1 mutants in the presence of Wnt3a CM. *E,* effects of LGR4 mutations on the stimulation of Wnt signaling. HEK293T cells were transfected with the LGR4 mutants, TOPFlash or FOPFlash firefly luciferase, and *Renilla* luciferase plasmids and were then stimulated with the CM of wild-type Rspo1 and Wnt3a.

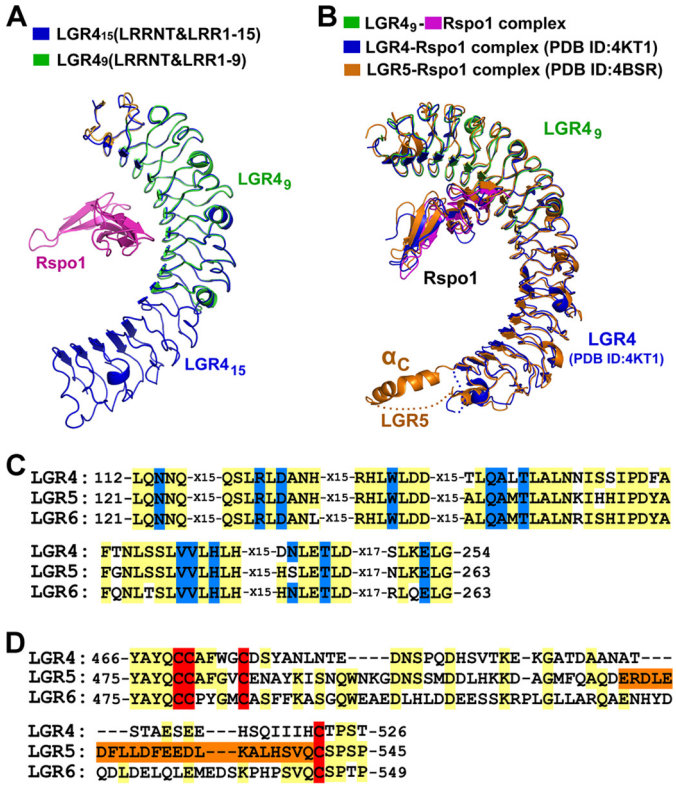

FIGURE 5. **Comparing LGR4 with LGR5 and LGR6.** *A,* structural comparison of Rspo1-bound LGR4$_9$ and ligand-free LGR4$_{15}$. LGR4$_9$ (LRRNT and LRR(1–9)) was superimposed with LGR4$_{15}$ (LRRNT and LRR(1–15)). The VLR modules in LGR4$_{15}$ and LGR4$_9$ were omitted in structural superimposition. LGR4$_9$ and Rspo1 are colored as in Fig. 2*B*. LGR4$_{15}$ is colored in *blue*. *B,* structural comparison of the LGR4$_9$-Rspo1 complex with the previously determined LGR4-Rspo1 and LGR5-Rspo1 structures. The LGR4$_9$-Rspo1 complex is colored in *green* (LGR4$_9$) and *purple* (Rspo1). The previously determined LGR4-Rspo1 and LGR5-Rspo1 structures are colored in *blue* and *orange*, respectively. *C,* sequence alignment of the Rspo1-binding residues. The Rspo1-binding residues are colored in *blue*. All the Rspo1-binding residues of LGR4 are conserved in LGR5 and LGR6. *D,* sequence alignment of the residues around α_C in the LRRCT regions. The cysteine residues of disulfide bonds in the LRRCT regions are colored in *red*. The sequence of the α_C helix of LGR5 is colored in *orange*.

We also mutated the interacting residues of LGR4 to evaluate their effects on the Rspo1 stimulation of Wnt signaling (Fig. 4*E*). Consistent with the mutational analysis of Rspo1, the mutations of Arg-135, Asn-226, and Thr-229/Glu-252 in LGR4, which interact with the nonconserved residues of Rspo1, had a minor effect on the Rspo1 stimulation of Wnt signaling. The double mutation (N114A/D137A) of Asn-114 and Asp-137 of LGR4, which interact with Arg-87 of Rspo1 in the hydrophilic binding region, severely affected the Rspo1 stimulation of Wnt signaling. The A181D/T183D and A181D/V204D mutations, which disrupt the hydrophobic binding region of LGR4, also completely abolished the Rspo1 stimulation of Wnt signaling. Therefore, both the electrostatic and hydrophobic interactions between Rspo1 and LGR4 are required for Rspo1 recognition by LGR4.

Comparison of LGR4 with LGR5 and LGR6—We further examined the conformational changes of LGR4 upon Rspo1 binding. The structure of the LGR4$_9$-Rspo1 complex was superimposed with ligand-free LGR4$_{15}$. As shown in Fig. 5, LRRNT and the central LRR1–9 repeats of LGR4$_9$ adopt identical conformations as those of LGR4$_{15}$ (Fig. 5*A*). The main chain and secondary structures of LGR4 do not undergo conformational changes upon Rspo1 binding, suggesting that LGR4 utilizes a rigid structural fold to recognize R-spondins to stimulate Wnt signaling. Our LGR4$_9$ and Rspo1 structures were also well superimposed with the previously determined LGR4-Rspo1 complex structure (PDB code 4KT1) (Fig. 5*B*) (21). All results of our luciferase assays for the LGR4 and Rspo1 mutations are consistent with the previously published data (20, 21), which further confirm our structures and mutagenesis analysis.

LGR5 and LGR6 serve as markers of specific stem cells and play important roles in stem cell maintenance. The ectodomains of LGR5 and LGR6 have significant sequence similarities to that of LGR4. Previous studies had reported the LGR5-Rpso1 complex structures (20). Structural comparison between LGR4 and LGR5 revealed that the ectodomain of LGR5 adopts a similar horseshoe-like structure as that of LGR4 (Fig. 5*B*). But the C-terminal LRRCT region of LGR5 contains an additional

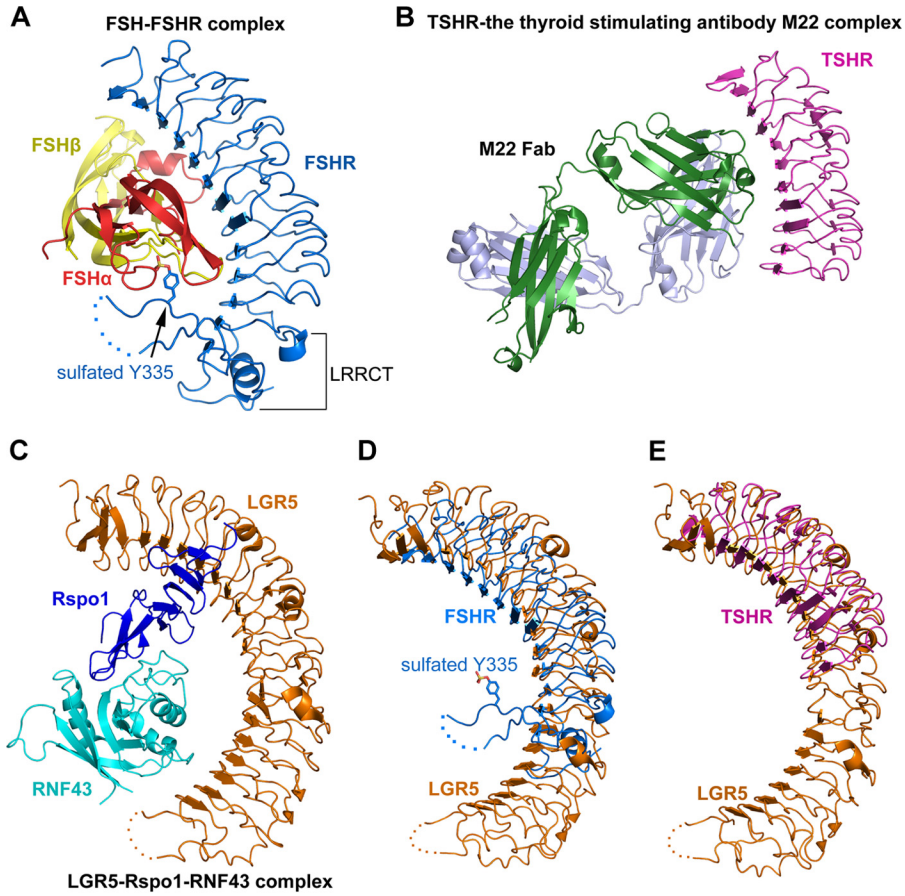

FIGURE 6. **Structural comparison of the receptor-ligand complexes of LGR1, LGR3, and LGR5.** *A,* crystal structure of FSH-FSHR (LGR1) complex (PDB code 4AY9). The α- and β-chain of FSH are colored in *red* and *yellow*, respectively. FSHR (LGR1) are colored in *blue*. The sulfated Tyr-335 is shown as *sticks*. The disordered region in the LRRCT/hinge region of FSHR is shown as *dashed lines*. *B,* crystal structure of TSHR (LGR3) in complex with the thyroid-stimulating antibody M22 (PDB code 3G04). The two chains of the M22 Fab are colored in *green* and *gray*, respectively. TSHR is colored in *purple*. *C,* crystal structure of the LGR5-Rspo1-RNF43 ternary complex (PDB code 4KNG). LGR5, Rspo1, and RNF43 are colored in *orange, blue,* and *cyan*, respectively. *D,* structural comparison of LGR5 with FSHR (LGR1). LGR5 and FSHR are colored in *orange* and *blue*, respectively. *E,* structural comparison of LGR5 with the M22-bound TSHR (LGR3). LGR5 and TSHR are colored in *orange* and *purple*, respectively.

α-helix (α_C), which mediated the dimerization of the LGR5-Rspo1 complex in crystals (details below) (20). Sequence alignment showed that the residues near the α_C region are not conserved in LGR4–6 (Fig. 5*D*).

Because all the Rspo1-interacting residues of LGR4 and LGR5 are conserved in LGR6 (Fig. 5*C*), LGR6 recognizes R-spondins through an identical surface as LGR4 and LGR5, which includes the central LRR4–9 repeats. All R-spondin proteins bind to the LGRs, but the binding affinity varies slightly among the members (30). Rspo1 exhibits ~40% sequence similarity with the other three members (7, 18). The critical LGR4-binding residues Arg-87, Phe-106, and Phe-110 of Rspo1 are conserved in the four R-spondin proteins (Fig. 3*B*). But the interacting residues Asp-85, Asn-109, and Lys-122 of Rspo1 are highly divergent in Rspo2–4 (Fig. 3*B*). Therefore, the limited difference in the binding affinities between Rspo1–4 and LGRs is likely determined by these variable interacting residues in the four R-spondins.

Divergence of Ligand Recognition by LGRs—To uncover the differences in ligand recognition, we structurally analyzed the molecular mechanisms of all LGRs. The molecular mechanisms of group A (LGR1–3) and group C receptors (LGR7–8) have been extensively studied. The complex structures of LGR1 (FSH receptor, FSHR) with FSH revealed that the heterodimeric FSH contains similarly β-folded α- and β-chains and is bound into the concave surface of LGR1 in a hand-clasp fashion (Fig. 6*A*) (39, 40). In addition, LGR1 provides a sulfotyrosine (sulfated Tyr-335) in the LRRCT/hinge region as a second interaction site with FSH (Fig. 6*A*). The concave surface in the LRR region of LGR1 represents a high affinity FSH-binding site. Interestingly, the monoclonal TSHR-stimulating antibody M22 also binds to the corresponding concave surface of LGR3 (TSHR) in the LGR3-M22 complex (Fig. 6*B*) (41), suggesting that the concave surface of LGR1 is the major binding site for FSH. The high affinity binding site of LGR1 was suggested to recruit FSH and mediate its conformational changes to form a sulfotyrosine-binding pocket for the sulfated Tyr-335 insertion. Tyr-335 of LGR1 is conserved in all group A receptors, and the tyrosine sulfation is also essential for the activation of LGR2 and LGR3 by luteinizing hormone and thyroid-stimulating hormone, respectively (42), suggesting that group A LGR universally utilizes the two-step mechanism of LGR1 for ligand recognition.

Relaxin and INSL3 are two-chain peptide hormones and play important roles in the control of adult fertility (43). Relaxin and INSL3 are specifically recognized by LGR7 and LGR8, respec-

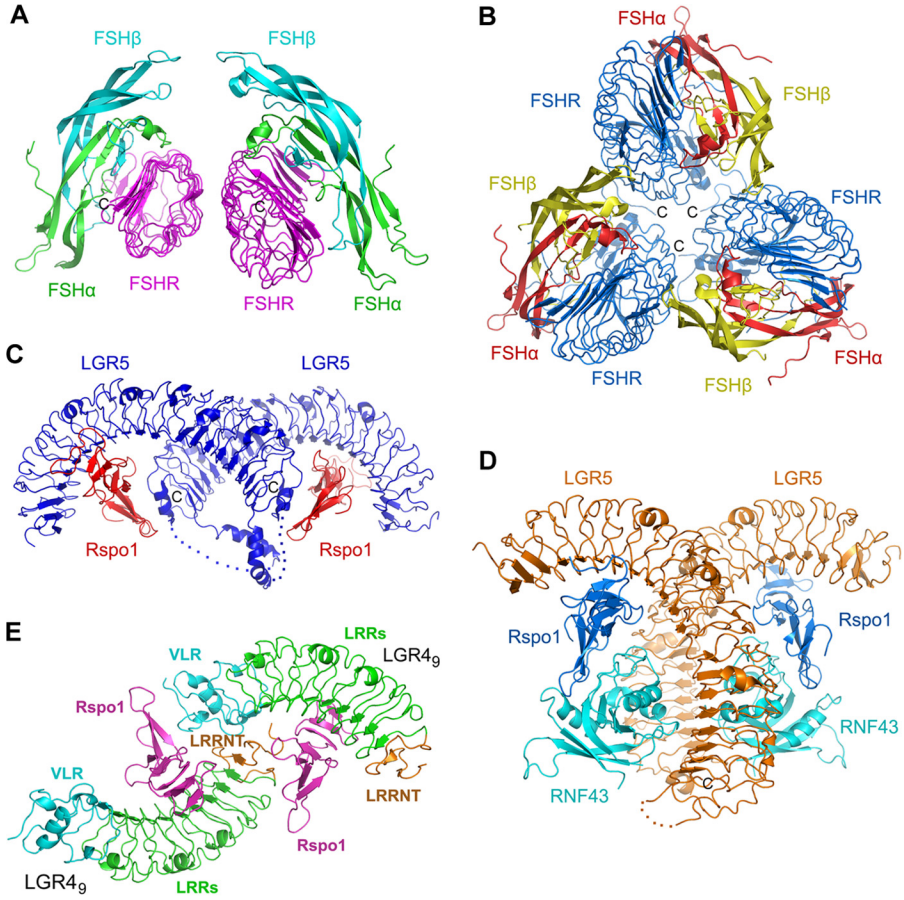

FIGURE 7. **Oligomerization of LGRs in crystals.** *A,* dimerization of FSH-FSHR complex in an asymmetric unit (PDB code 1XWD). The LRRCT/hinge-truncated ectodomain of FSHR is colored in *purple*. The α- and β-chain of FSH are colored in *green* and *cyan*, respectively. *B,* trimerization of FSH-FSHR complex in an asymmetric unit (PDB code 4AY9). The entire ectodomain of FSHR is colored in *blue*. The α- and β-chains of FSH are colored in *red* and *yellow*, respectively. *C,* dimerization of the LGR5-Rspo1 binary complex in an asymmetric unit (PDB code 4BSR). LGR5 and Rspo1 are colored in *blue* and *red,* respectively. The disordered loops in the LRRCT region of LGR5 are shown as *dashed lines*. *D,* dimerization of the LGR5-Rspo1-RNF43 ternary complex in an asymmetric unit (PDB code 4KNG). LGR5, Rspo1, and RNF43 are colored in *orange, blue,* and *cyan*, respectively. *E,* two LGR4$_9$-Rspo1 copies in an asymmetric unit in our complex structure. The two LGR4-Rspo1 copies interact with each other via the engineered VLR module and the LRRNT region.

tively (44). Distinct from R-spondins and FSH, Relaxin and INSL3 are α-folded heterodimers of A- and B-chain linked by disulfide bonds, which are structurally similar to insulin. Previous biochemical studies had revealed that the recognition of relaxin and INSL3 by LGR7 and LGR8 requires multiple interactions between the ligands and various receptor domains. The primary binding occurs via the interactions between B-chain of relaxin/INSL3 with the inner β-sheets of the LRRs in the ectodomains of LGR7 and LGR8 (45, 46). The primary binding site provides a high affinity interface for the ligands. A secondary low affinity binding site is located at the extracellular loops in the 7TM domains of LGR7 and LGR8, which binds the A chains of relaxin and INSL3 (47, 48). Therefore, both the LRR regions and the 7TM extracellular loops are involved in the relaxin/INSL3 recognition by LGR7 and LGR8, suggesting a unique multiple-interface mechanism of group C receptors.

Our LGR4-Rspo1 complex structure and previously determined LGR4–5 structures revealed that the LRR region of LGR4 is the sole binding site for Rspo1, suggesting that LGR4–6 recognize R-spondins via a one-site binding mechanism (Fig. 2) (20, 21). Although the transmembrane E3 ubiquitin ligase ZNRF3 and its homologue RNF43 were reported to interact with R-spondins and form complexes with LGR4–6 (49, 50), the LGR5-Rspo1-RNF43 ternary complex structure demonstrated that LGR5 does not interact with RNF43 to affect Rspo1 binding (Fig. 6*C*) (19). In addition, LGR5 contains more redundancy of LRR repeats than LGR1 and LGR3 (Fig. 6, *D* and *E*). The distinct one-site binding mechanism of R-spondin recognition by LGR4–6, together with the structural differences between LGR5 and LGR1, suggests the mechanism divergence in ligand recognition of LGRs.

Potential Oligomerization of LGRs in Ligand Recognition—It was suggested that glycoprotein hormone receptors undergo dimerization in living cells (51, 52). The complex of FSH and LGR1 without the LRRCT/hinge region was demonstrated to form a dimer at high concentration in solution (39). The crystal structure of FSH with the hinge-truncated LGR1 revealed that the dimer was formed by two FSH-LGR1 complex molecules via three β-strands on the convex surface of LGR1 in an asymmetric unit (Fig. 7*A*). The small dimerization interface indicated the weak interactions between the two protomers (Fig. 7*A*), consistent with that the dimerization was just detected by the chemical cross-linking assays (39). In addition, recent studies suggested that LGR1 underwent trimerization upon FSH binding when the conserved Tyr-335 residue in the LRRCT/hinge domain was sulfated (Fig. 7*B*) (40, 53). The trimerization

of LGR1 provided an additional binding site for FSH, which involves the interaction of the convex surface of LGR1 with a neighboring FSH (40). The trimerization was also observed in the crystals of LGR1 with FSH that was deglycosylated at Asn-52 in the α-chain (53). As the trimerization buried a large surface area of each protomer, the FSH-binding capacity of LGR1 was increased to 3-fold for the deglycosylated FSH (53). Although the trimer model of LGR1 in FSH recognition could well explain some observation in biochemical and functional studies (53), the *in vivo* relevance of the LGR1-FSH trimerization and the actual oligomerization form in living cells still need to be determined.

Dimerization of the LGR5-Rspo1 complex was also observed in crystals, although LGR5 formed a 1:1 complex with Rspo1 in solution (Fig. 7*C*) (20). In the LGR5-Rspo1 binary complex structure (PDB code 4BSR and space group $P22_12_1$) (20), the dimerization of the LGR5-Rspo1 complex was mediated by the LGR5 α_C-helices and the Rspo1-LGR5 LRRCT interactions, forming a cross-dimer of LGR5-Rspo1 complex in an asymmetric unit (Fig. 7*C*). But in the LGR5-Rspo1-RNF43 ternary complex structure (19) (PDB code 4KNG and space group $P2_12_12_1$), a back-to-back dimer of the LGR5-Rspo1-RNF43 complex was formed by the LGR5-LGR5 and LGR5-RNF43 trans-interactions (Fig. 7*D*). It is unknown which form of dimerization functions in cells and whether the two dimerization forms represent different states of LGR5 during ligand recognition. Different from the LGR5-Rspo1 complex, the LGR4-Rspo1 complex did not dimerize in the previously determined structure (21) and our structures. The previously determined LGR4-Rspo1 structure (PDB code 4KT1 and space group $P3_2$) only contained one LGR4-Rspo1 molecule in an asymmetric unit. Although there are two LGR4-Rspo1 molecules in our structure, the two copies do not form a real dimer because the two copies interact with each other via the engineered VLR module and the LRRNT region (Fig. 7*E*).

Interestingly, *Xenopus* LGR4 was found to dimerize both in solution and in crystals (22). The dimerization of *Xenopus* LGR4 was mediated by the side-by-side interactions between LRRNT and the first four LRRs of the two LGR4 copies in an asymmetric unit, forming a tail-to-tail dimer in an asymmetric unit (22). But our human $LGR4_{15}$, which contains the intact LRRNT and the first four LRR repeats, did not dimerize either in solution or in crystals. Given that human LGR4 has significant sequence similarities to that of *Xenopus*, it is possible that the C-terminal engineered VLR module of $LGR4_{15}$ has negative effects on the human LGR4 dimerization. LGR7 and LGR8 were also reported to homodimerize and heterodimerize in cells, which regulated the negative cooperativity in relaxin/INSL3 binding (54). Dimerization and negative cooperativity in ligand binding have been generally demonstrated for the insulin receptor (55), β2-adrenergic receptor (56), and chemokine receptors (57). It will be interesting to investigate the negative cooperativity in R-spondin binding and its correlation with the dimerization of LGR4–6. Taken together, LGRs likely undergo different types of oligomerization during ligand recognition.

Closing Remarks—LGR4–6 receptors are important for stem cell maintenance by stimulating Wnt signaling. It is important to uncover the molecular mechanism of R-spondin recognition by LGR4–6. In this study, we utilized the hybrid LRR technique to obtain functional human LGR4 proteins, and we determined the crystal structure of the LGR4-Rspo1 complex. Our studies, together with previous reports, suggest that LGR4–6 recognize R-spondins via a one-site binding mechanism, which involves the electrostatic and hydrophobic interactions between R-spondins and the concave surface in the LRR region of LGR4–6. Our analysis reveals the structural differences of the three groups of LGRs in ligand recognition, highlighting the divergence in the mechanisms of ligand recognition. Because of the important roles of LGR4–6 receptors and R-spondin proteins in embryonic development and in many human diseases, our structures are important for potential drug design.

Acknowledgments—We thank the staff at the Shanghai Synchrotron Radiation Facility (Shanghai, China) for assistance with data collection. We also thank members of the Zhu laboratory for helpful discussions and technical assistance.

REFERENCES

1. Luo, C. W., and Hsueh, A. J. (2006) Genomic analyses of the evolution of LGR genes. *Chang Gung Med. J.* **29,** 2–8
2. Barker, N., Tan, S., and Clevers, H. (2013) Lgr proteins in epithelial stem cell biology. *Development* **140,** 2484–2494
3. Van Loy, T., Vandersmissen, H. P., Van Hiel, M. B., Poels, J., Verlinden, H., Badisco, L., Vassart, G., and Vanden Broeck, J. (2008) Comparative genomics of leucine-rich repeats containing G protein-coupled receptors and their ligands. *Gen. Comp. Endocrinol.* **155,** 14–21
4. Hsu, S. Y., Kudo, M., Chen, T., Nakabayashi, K., Bhalla, A., van der Spek, P. J., van Duin, M., and Hsueh, A. J. (2000) The three subfamilies of leucine-rich repeat-containing G protein-coupled receptors (LGR): identification of LGR6 and LGR7 and the signaling mechanism for LGR7. *Mol. Endocrinol.* **14,** 1257–1271
5. Clevers, H., and Nusse, R. (2012) Wnt/β-catenin signaling and disease. *Cell* **149,** 1192–1205
6. Niehrs, C. (2012) The complex world of WNT receptor signalling. *Nat. Rev. Mol. Cell Biol.* **13,** 767–779
7. Kim, K. A., Zhao, J., Andarmani, S., Kakitani, M., Oshima, T., Binnerts, M. E., Abo, A., Tomizuka, K., and Funk, W. D. (2006) R-Spondin proteins: a novel link to β-catenin activation. *Cell Cycle* **5,** 23–26
8. Jin, Y. R., and Yoon, J. K. (2012) The R-spondin family of proteins: emerging regulators of WNT signaling. *Int. J. Biochem. Cell Biol.* **44,** 2278–2287
9. Kazanskaya, O., Glinka, A., del Barco Barrantes, I., Stannek, P., Niehrs, C., and Wu, W. (2004) R-Spondin2 is a secreted activator of Wnt/β-catenin signaling and is required for Xenopus myogenesis. *Dev. Cell* **7,** 525–534
10. Schuijers, J., and Clevers, H. (2012) Adult mammalian stem cells: the role of Wnt, Lgr5, and R-spondins. *EMBO J.* **31,** 2685–2696
11. Parma, P., Radi, O., Vidal, V., Chaboissier, M. C., Dellambra, E., Valentini, S., Guerra, L., Schedl, A., and Camerino, G. (2006) R-spondin1 is essential in sex determination, skin differentiation and malignancy. *Nat. Genet.* **38,** 1304–1309
12. Bell, S. M., Schreiner, C. M., Wert, S. E., Mucenski, M. L., Scott, W. J., and Whitsett, J. A. (2008) R-spondin 2 is required for normal laryngeal-tracheal, lung, and limb morphogenesis. *Development* **135,** 1049–1058
13. Aoki, M., Mieda, M., Ikeda, T., Hamada, Y., Nakamura, H., and Okamoto, H. (2007) R-spondin3 is required for mouse placental development. *Dev. Biol.* **301,** 218–226
14. Blaydon, D. C., Ishii, Y., O'Toole, E. A., Unsworth, H. C., Teh, M. T., Rüschendorf, F., Sinclair, C., Hopsu-Havu, V. K., Tidman, N., Moss, C., Watson, R., de Berker, D., Wajid, M., Christiano, A. M., and Kelsell, D. P. (2006) The gene encoding R-spondin 4 (RSPO4), a secreted protein implicated in Wnt signaling, is mutated in inherited anonychia. *Nat. Genet.* **38,** 1245–1247

15. Bergmann, C., Senderek, J., Anhuf, D., Thiel, C. T., Ekici, A. B., Poblete-Gutierrez, P., van Steensel, M., Seelow, D., Nürnberg, G., Schild, H. H., Nürnberg, P., Reis, A., Frank, J., and Zerres, K. (2006) Mutations in the gene encoding the Wnt-signaling component R-spondin 4 (RSPO4) cause autosomal recessive anonychia. *Am. J. Hum. Genet.* **79,** 1105–1109
16. de Lau, W., Barker, N., Low, T. Y., Koo, B. K., Li, V. S., Teunissen, H., Kujala, P., Haegebarth, A., Peters, P. J., van de Wetering, M., Stange, D. E., van Es, J. E., Guardavaccaro, D., Schasfoort, R. B., Mohri, Y., Nishimori, K., Mohammed, S., Heck, A. J., and Clevers, H. (2011) Lgr5 homologues associate with Wnt receptors and mediate R-spondin signalling. *Nature* **476,** 293–297
17. Glinka, A., Dolde, C., Kirsch, N., Huang, Y. L., Kazanskaya, O., Ingelfinger, D., Boutros, M., Cruciat, C. M., and Niehrs, C. (2011) LGR4 and LGR5 are R-spondin receptors mediating Wnt/β-catenin and Wnt/PCP signalling. *EMBO Rep.* **12,** 1055–1061
18. Kim, K. A., Wagle, M., Tran, K., Zhan, X., Dixon, M. A., Liu, S., Gros, D., Korver, W., Yonkovich, S., Tomasevic, N., Binnerts, M., and Abo, A. (2008) R-Spondin family members regulate the Wnt pathway by a common mechanism. *Mol. Biol. Cell* **19,** 2588–2596
19. Chen, P. H., Chen, X., Lin, Z., Fang, D., and He, X. (2013) The structural basis of R-spondin recognition by LGR5 and RNF43. *Genes Dev.* **27,** 1345–1350
20. Peng, W. C., de Lau, W., Forneris, F., Granneman, J. C., Huch, M., Clevers, H., and Gros, P. (2013) Structure of stem cell growth factor R-spondin 1 in complex with the ectodomain of its receptor LGR5. *Cell Rep.* **3,** 1885–1892
21. Wang, D., Huang, B., Zhang, S., Yu, X., Wu, W., and Wang, X. (2013) Structural basis for R-spondin recognition by LGR4/5/6 receptors. *Genes Dev.* **27,** 1339–1344
22. Xu, K., Xu, Y., Rajashankar, K. R., Robev, D., and Nikolov, D. B. (2013) Crystal structures of Lgr4 and its complex with R-spondin1. *Structure* **21,** 1683–1689
23. Otwinowski, Z., and Minor, W. (1997) Processing of x-ray diffraction data collected in oscillation mode. *Methods Enzymol.* **276,** 307–326
24. Yoon, S. I., Kurnasov, O., Natarajan, V., Hong, M., Gudkov, A. V., Osterman, A. L., and Wilson, I. A. (2012) Structural basis of TLR5-flagellin recognition and signaling. *Science* **335,** 859–864
25. McCoy, A. J., Grosse-Kunstleve, R. W., Adams, P. D., Winn, M. D., Storoni, L. C., and Read, R. J. (2007) Phaser crystallographic software. *J. Appl. Crystallogr.* **40,** 658–674
26. Collaborative Computation Project No. 4 (1994) The CCP4 suite: programs for protein crystallography. *Acta Crystallogr. D. Biol. Crystallogr.* **50,** 760–763
27. Murshudov, G. N., Vagin, A. A., and Dodson, E. J. (1997) Refinement of macromolecular structures by the maximum-likelihood method. *Acta Crystallogr. D. Biol. Crystallogr.* **53,** 240–255
28. Emsley, P., and Cowtan, K. (2004) Coot: model-building tools for molecular graphics. *Acta Crystallogr. D. Biol. Crystallogr.* **60,** 2126–2132
29. Laskowski, A. R., MacArthur, W. M., Moss, S. D., and Thornton, M. J. (1993) PROCHECK: a program to check the stereochemical quality of protein structures. *J. Appl. Cryst.* **26,** 283–291
30. Carmon, K. S., Gong, X., Lin, Q., Thomas, A., and Liu, Q. (2011) R-spondins function as ligands of the orphan receptors LGR4 and LGR5 to regulate Wnt/β-catenin signaling. *Proc. Natl. Acad. Sci. U.S.A.* **108,** 11452–11457
31. Kim, H. M., Park, B. S., Kim, J. I., Kim, S. E., Lee, J., Oh, S. C., Enkhbayar, P., Matsushima, N., Lee, H., Yoo, O. J., and Lee, J. O. (2007) Crystal structure of the TLR4-MD-2 complex with bound endotoxin antagonist Eritoran. *Cell* **130,** 906–917
32. Holm, L., and Rosenström, P. (2010) Dali server: conservation mapping in 3D. *Nucleic Acids Res.* **38,** W545–W549
33. Jin, M. S., Kim, S. E., Heo, J. Y., Lee, M. E., Kim, H. M., Paik, S. G., Lee, H., and Lee, J. O. (2007) Crystal structure of the TLR1-TLR2 heterodimer induced by binding of a tri-acylated lipopeptide. *Cell* **130,** 1071–1082
34. Mosyak, L., Wood, A., Dwyer, B., Buddha, M., Johnson, M., Aulabaugh, A., Zhong, X., Presman, E., Benard, S., Kelleher, K., Wilhelm, J., Stahl, M. L., Kriz, R., Gao, Y., Cao, Z., Ling, H. P., Pangalos, M. N., Walsh, F. S., and Somers, W. S. (2006) The structure of the Lingo-1 ectodomain, a module implicated in central nervous system repair inhibition. *J. Biol. Chem.* **281,** 36378–36390
35. Raz, E., Schejter, E. D., and Shilo, B. Z. (1991) Interallelic complementation among DER/flb alleles: implications for the mechanism of signal transduction by receptor-tyrosine kinases. *Genetics* **129,** 191–201
36. Eigenbrot, C., Ultsch, M., Dubnovitsky, A., Abrahmsén, L., and Härd, T. (2010) Structural basis for high affinity HER2 receptor binding by an engineered protein. *Proc. Natl. Acad. Sci. U.S.A.* **107,** 15039–15044
37. Cho, H. S., and Leahy, D. J. (2002) Structure of the extracellular region of HER3 reveals an interdomain tether. *Science* **297,** 1330–1333
38. Bouyain, S., Longo, P. A., Li, S., Ferguson, K. M., and Leahy, D. J. (2005) The extracellular region of ErbB4 adopts a tethered conformation in the absence of ligand. *Proc. Natl. Acad. Sci. U.S.A.* **102,** 15024–15029
39. Fan, Q. R., and Hendrickson, W. A. (2005) Structure of human follicle-stimulating hormone in complex with its receptor. *Nature* **433,** 269–277
40. Jiang, X., Liu, H., Chen, X., Chen, P. H., Fischer, D., Sriraman, V., Yu, H. N., Arkinstall, S., and He, X. (2012) Structure of follicle-stimulating hormone in complex with the entire ectodomain of its receptor. *Proc. Natl. Acad. Sci. U.S.A.* **109,** 12491–12496
41. Sanders, J., Chirgadze, D. Y., Sanders, P., Baker, S., Sullivan, A., Bhardwaja, A., Bolton, J., Reeve, M., Nakatake, N., Evans, M., Richards, T., Powell, M., Miguel, R. N., Blundell, T. L., Furmaniak, J., and Smith, B. R. (2007) Crystal structure of the TSH receptor in complex with a thyroid-stimulating autoantibody. *Thyroid* **17,** 395–410
42. Costagliola, S., Panneels, V., Bonomi, M., Koch, J., Many, M. C., Smits, G., and Vassart, G. (2002) Tyrosine sulfation is required for agonist recognition by glycoprotein hormone receptors. *EMBO J.* **21,** 504–513
43. Hsu, S. Y., Nakabayashi, K., Nishi, S., Kumagai, J., Kudo, M., Bathgate, R. A., Sherwood, O. D., and Hsueh, A. J. (2003) Relaxin signaling in reproductive tissues. *Mol. Cell. Endocrinol.* **202,** 165–170
44. Hsu, S. Y., Nakabayashi, K., Nishi, S., Kumagai, J., Kudo, M., Sherwood, O. D., and Hsueh, A. J. (2002) Activation of orphan receptors by the hormone relaxin. *Science* **295,** 671–674
45. Scott, D. J., Wilkinson, T. N., Zhang, S., Ferraro, T., Wade, J. D., Tregear, G. W., and Bathgate, R. A. (2007) Defining the LGR8 residues involved in binding insulin-like peptide 3. *Mol. Endocrinol.* **21,** 1699–1712
46. Büllesbach, E. E., and Schwabe, C. (2005) The trap-like relaxin-binding site of the leucine-rich G-protein-coupled receptor 7. *J. Biol. Chem.* **280,** 14051–14056
47. Sudo, S., Kumagai, J., Nishi, S., Layfield, S., Ferraro, T., Bathgate, R. A., and Hsueh, A. J. (2003) H3 relaxin is a specific ligand for LGR7 and activates the receptor by interacting with both the ectodomain and the exoloop 2. *J. Biol. Chem.* **278,** 7855–7862
48. Diepenhorst, N. A., Petrie, E. J., Chen, C. Z., Wang, A., Hossain, M. A., Bathgate, R. A., and Gooley, P. R. (2014) Investigation of interactions at the extracellular loops of the relaxin family peptide receptor 1 (RXFP1). *J. Biol. Chem.* **289,** 34938–34952
49. Hao, H. X., Xie, Y., Zhang, Y., Charlat, O., Oster, E., Avello, M., Lei, H., Mickanin, C., Liu, D., Ruffner, H., Mao, X., Ma, Q., Zamponi, R., Bouwmeester, T., Finan, P. M., Kirschner, M. W., Porter, J. A., Serluca, F. C., and Cong, F. (2012) ZNRF3 promotes Wnt receptor turnover in an R-spondin-sensitive manner. *Nature* **485,** 195–200
50. Koo, B. K., Spit, M., Jordens, I., Low, T. Y., Stange, D. E., van de Wetering, M., van Es, J. H., Mohammed, S., Heck, A. J., Maurice, M. M., and Clevers, H. (2012) Tumour suppressor RNF43 is a stem-cell E3 ligase that induces endocytosis of Wnt receptors. *Nature* **488,** 665–669
51. Roess, D. A., Horvat, R. D., Munnelly, H., and Barisas, B. G. (2000) Luteinizing hormone receptors are self-associated in the plasma membrane. *Endocrinology* **141,** 4518–4523
52. Horvat, R. D., Barisas, B. G., and Roess, D. A. (2001) Luteinizing hormone receptors are self-associated in slowly diffusing complexes during receptor desensitization. *Mol. Endocrinol.* **15,** 534–542
53. Jiang, X., Fischer, D., Chen, X., McKenna, S. D., Liu, H., Sriraman, V., Yu, H. N., Goutopoulos, A., Arkinstall, S., and He, X. (2014) Evidence for follicle-stimulating hormone receptor as a functional trimer. *J. Biol. Chem.* **289,** 14273–14282

54. Svendsen, A. M., Vrecl, M., Knudsen, L., Heding, A., Wade, J. D., Bathgate, R. A., De Meyts, P., and Nøhr, J. (2009) Dimerization and negative cooperativity in the relaxin family peptide receptors. *Ann. N.Y. Acad. Sci.* **1160,** 54–59
55. de Meyts, P., Roth, J., Neville, D. M., Jr., Gavin, J. R., 3rd, and Lesniak, M. A. (1973) Insulin interactions with its receptors: experimental evidence for negative cooperativity. *Biochem. Biophys. Res. Commun.* **55,** 154–161
56. Limbird, L. E., Meyts, P. D., and Lefkowitz, R. J. (1975) β-Adrenergic receptors: evidence for negative cooperativity. *Biochem. Biophys. Res. Commun.* **64,** 1160–1168
57. Springael, J. Y., Urizar, E., and Parmentier, M. (2005) Dimerization of chemokine receptors and its functional consequences. *Cytokine Growth Factor Rev.* **16,** 611–623